figure S1

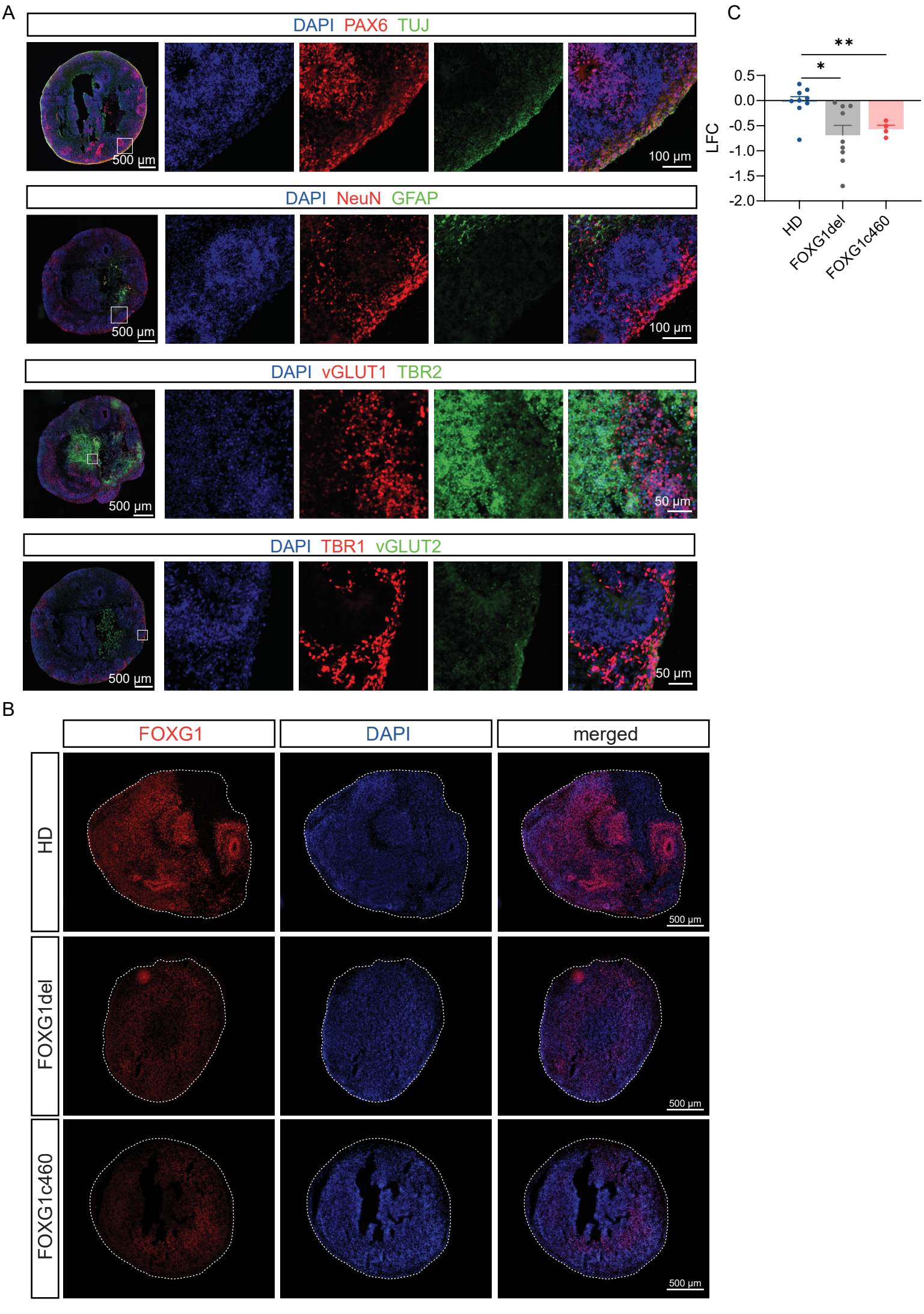

A
DAPI PAX6 TUJ
500 µm
100 µm
DAPI NeuN GFAP
500 µm
100 µm
DAPI vGLUT1 TBR2
500 µm
50 µm
DAPI TBR1 vGLUT2
500 µm
50 µm
C
**
*
0.5
0.0
-0.5
-1.0
-1.5
-2.0
LFC
HD
FOXG1del
FOXG1c460
B
FOXG1
DAPI
merged
HD
FOXG1del
FOXG1c460
500 µm
500 µm
500 µm

Fig. S1: Characterisation of human brain organoids and expression of FOXG1

(A) Immunostainings of control organoid slices after 105 days in culture presenting different markers (Paired box protein (PAX6), Neuron-specific class III beta-tubulin (TUJ), neuronal nuclei (NeuN), glial fibrillary acidic protein (GFAP), vesicular glutamate transporter 1 (vGLUT1), vGLUT2, T-box brain transcription factor 1 (TBR1), TBR2) of neural development. Scale bars as indicated in the figures.

(B) Immunostainings of FOXG1 in CO of healthy donor (HD), FOXG1del, and FOXG1c460 showing reduced FOXG1 protein expression in FOXG1del and FOXG1c460 compared to HD after 105 d in culture. Dashed line delineates the organoid surface. Scale bars as indicated in the figure.

(C) RT-qPCR results of *FOXG1* expression in healthy donor (HD), FOXG1del, and FOXG1c460 d105 hCOs, showing reduced *FOXG1* expression upon the mutations (with the housekeeping gene ACTIN B (*ACTB*) as reference). The fold change in expression in FOXG1del and FOXG1c460 hCO is compared to that in control organoids. Statistical analysis was performed using One-way ANOVA test, *: $p < 0.05$, **: $p<0.01$. n=4-9.

figure S2

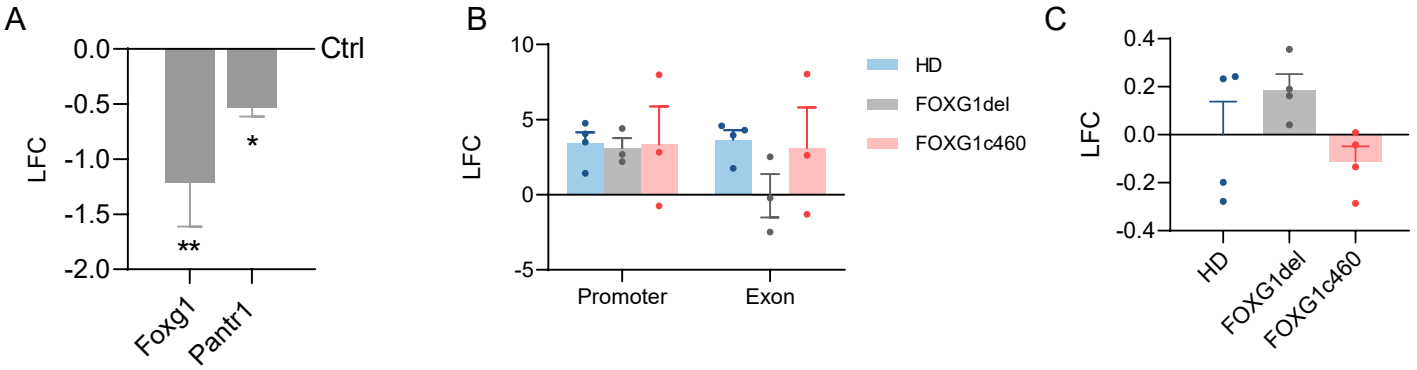

A
0.0
-0.5
-1.0
-1.5
-2.0
LFC
Ctrl
**
*
Foxg1
Pantr1
B
10
5
0
-5
LFC
Promoter
Exon
HD
FOXG1del
FOXG1c460
C
0.4
0.2
0.0
-0.2
-0.4
LFC
HD
FOXG1del
FOXG1c460

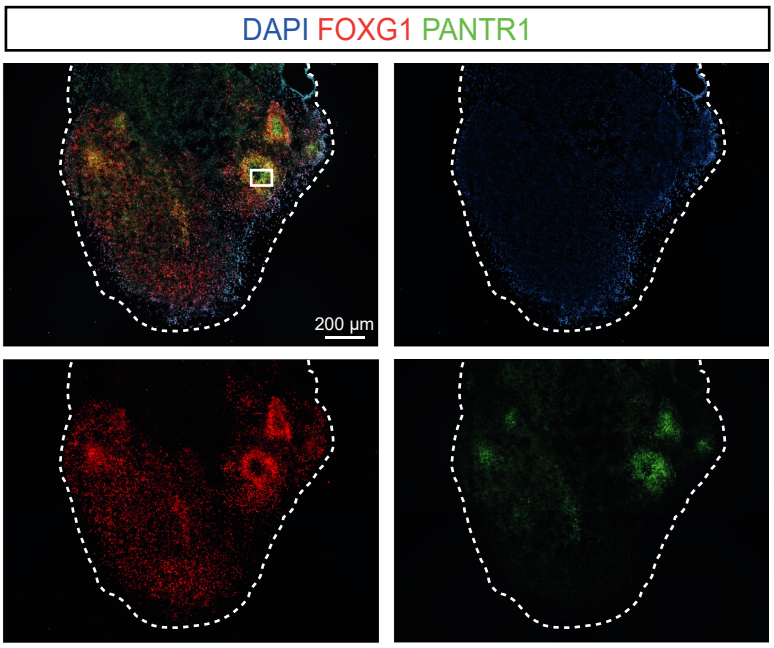
Fig. S2: FOXG1 regulates *Pantr1* expression in mice and humans

(A) *Foxg1* and *Pantr1* expression in *Foxg1*$^{cre/+}$ adult hippocampus tissue compared to wildtype mice (WT). Shown is the $\log_2$(foldchange) (LFC). *Gapdh* was used as housekeeping gene. Results of qPCRs are shown as mean ± SEM. P-values were calculated using unpaired, two tailed Student's t-test: *p < 0.05, **p < 0.01. n=3.

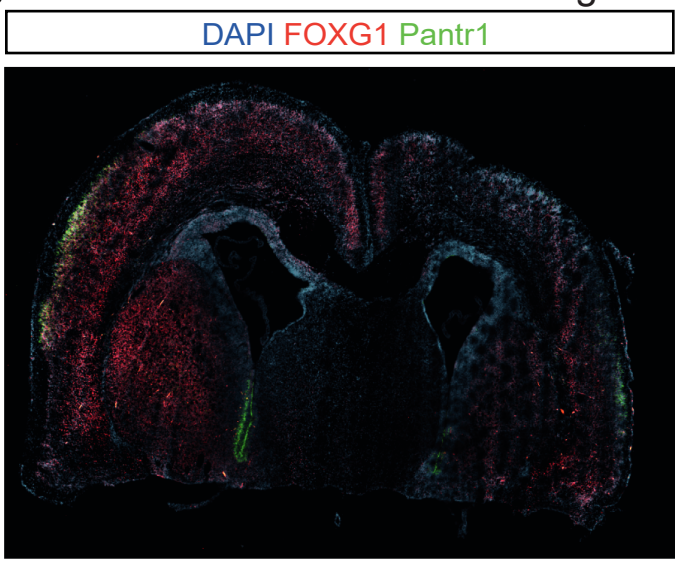
(B) ChIP-qPCR analysis of FOXG1 binding at the *PANTR1* promoter and exon regions in human cortical organoids (hCO) from healthy donor (HD), FOXG1del, and FOXG1c460 genotypes. FOXG1 enrichment is shown as $\log_2$ fold change (LFC) relative to IgG controls. No significant differences in FOXG1 binding were observed between genotypes. Data are presented as mean ± SEM; n = 3–4 organoids per group.

(C) RT-qPCR analysis of *PANTR1* expression in hCOs from HD, FOXG1del, and FOXG1c460 genotypes. A mild reduction in *PANTR1* expression is observed in FOXG1c460 samples. Data are shown as $\log_2$ fold change (LFC) relative to HD (mean ± SEM); n = 3–4 organoids per group.

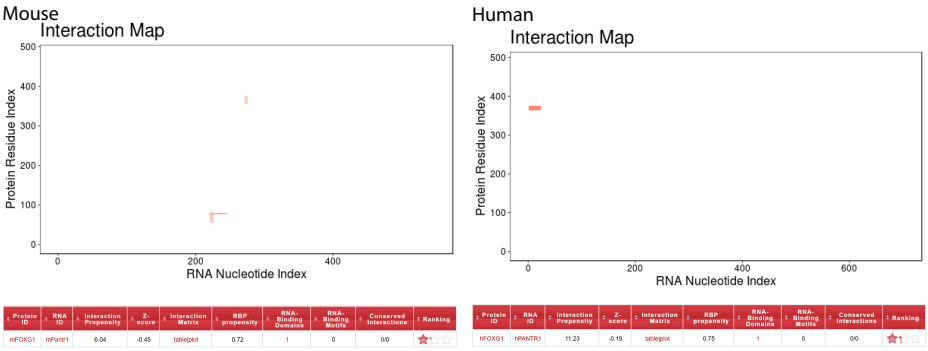
A


DAPI FOXG1 PANTR1
200 µm

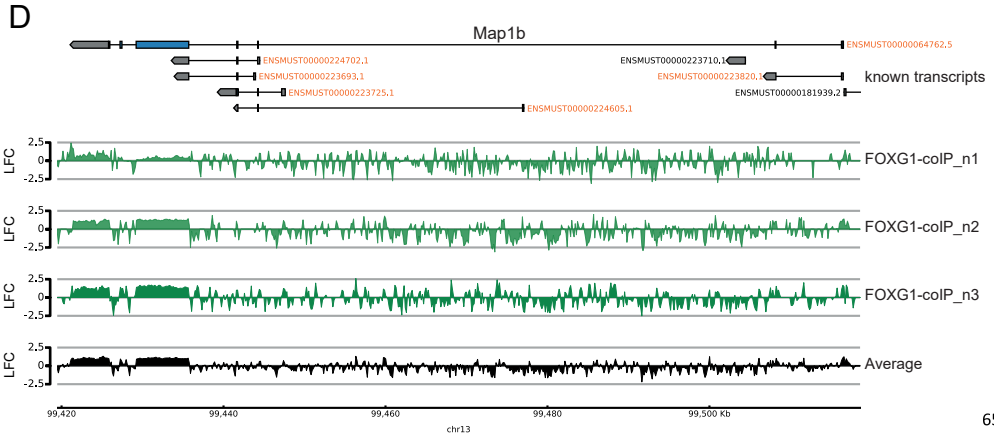
B


DAPI FOXG1 Pantr1

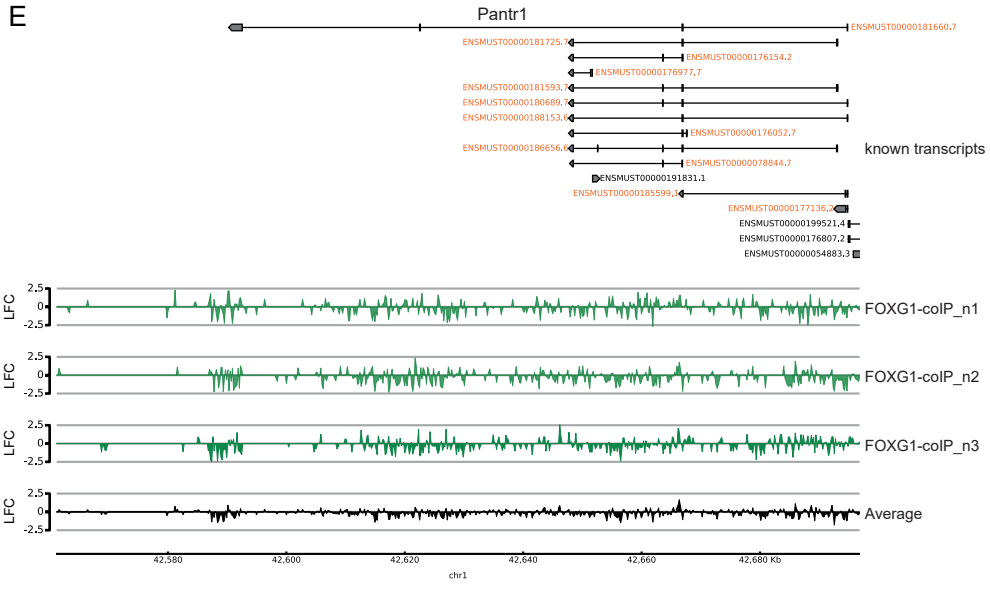
C


Mouse
Interaction Map
Protein Residue Index
RNA Nucleotide Index
Human
Interaction Map
Protein Residue Index
RNA Nucleotide Index

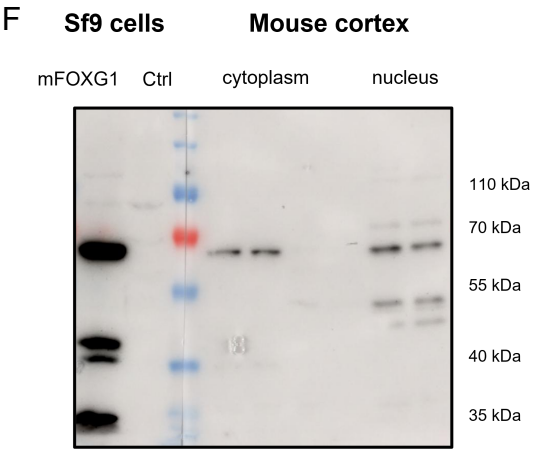
D


Map1b
known transcripts
FOXG1-coIP_n1
FOXG1-coIP_n2
FOXG1-coIP_n3
Average
LFC
chr13

E


Pantr1
known transcripts
FOXG1-coIP_n1
FOXG1-coIP_n2
FOXG1-coIP_n3
Average
LFC
chr1

F


Sf9 cells
Mouse cortex
mFOXG1
Ctrl
cytoplasm
nucleus
110 kDa
70 kDa
55 kDa
40 kDa
35 kDa

G

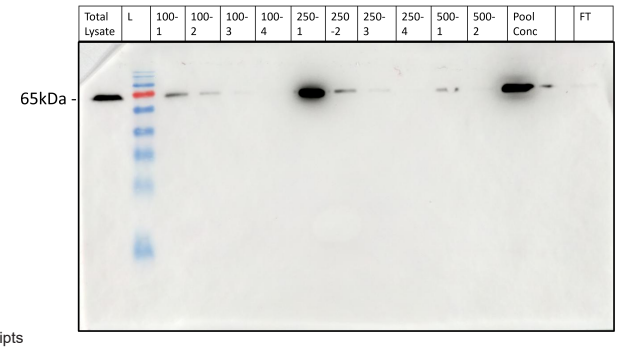

Total Lysate
L
100-1
100-2
100-3
100-4
250-1
250-2
250-3
250-4
500-1
500-2
Pool Conc
FT
65kDa

Fig. S3: FOXG1 localises in the vicinity of *PANTR1 in vivo*

(A) Overview of the expression of *PANTR1* (smFISH) and FOXG1 protein in human d105 brain organoids. The boxed area indicates the magnification shown in Fig. 4F.

(B) Overview of the expression of *Pantr1* (smFISH) and FOXG1 protein in the mouse brain.

(C) *In silico* prediction of FOXG1–*Pantr1* RNA–protein interactions using catRAPID. Interaction maps for mouse (left) and human (right) show predicted contact regions between FOXG1 protein residues (y-axis) and *Pantr1* RNA nucleotides (x-axis). Heatmap intensity indicates interaction propensity. Tables below each map summarise interaction parameters, including interaction strength (Z-score), RNA- and RBP-binding propensity, and region-specific details. In both species, FOXG1 is predicted to bind *Pantr1* RNA with high confidence, despite lacking canonical RNA-binding domains.

(D) Upper part: Different transcript variants of *Map1b* (orange). Boxes represent the different exons. Lower part: RIPseq tracks of $\log_2$(foldchange) (LFC) of reads in FOXG1-coIP vs IgG-coIP in the different n (green) and the average of those LFCs (black) in the genomic region of *Map1b*. On the x-axis the position on the corresponding chromosome is indicated in bp of the mm10 genome.

(E) Upper part: Different transcript variants of *Pantr1* (orange). Boxes represent the different exons. Lower part: RIPseq tracks of $\log_2$(foldchange) (LFC) of reads in FOXG1-coIP vs IgG-coIP in the different n (green) and the average of those LFCs (black) in the genomic region of *Pantr1*. On the x-axis the position on the corresponding chromosome is indicated in bp of the mm10 genome.

(F) Immunoblot analysis of recombinant mouse FOXG1 (mFOXG1) expressed in Sf9 cells and endogenous FOXG1 in cytoplasmic and nuclear fractions of mouse cortex. The mFOXG1 lane confirms the expected molecular weight and antibody specificity. In the mouse cortex, FOXG1 is predominantly detected in the nuclear fraction, with multiple bands suggesting post-translational modifications or isoforms. Ctrl: untransfected Sf9 cell lysate. Molecular weight markers are indicated on the right.

(G) Immunoblot showing mouse FOXG1 protein detection in elution fractions collected during recombinant FOXG1 purification. Elution was performed using increasing imidazole concentrations (100–500 mM), and individual fractions are indicated above each lane. A strong FOXG1 signal is observed in the 250 mM elution fractions. The pooled and concentrated fractions (Pool Conc) show successful enrichment of FOXG1 at ~65 kDa. L: ladder; FT: flow-through; Total Lysate: input before purification.

figure S4

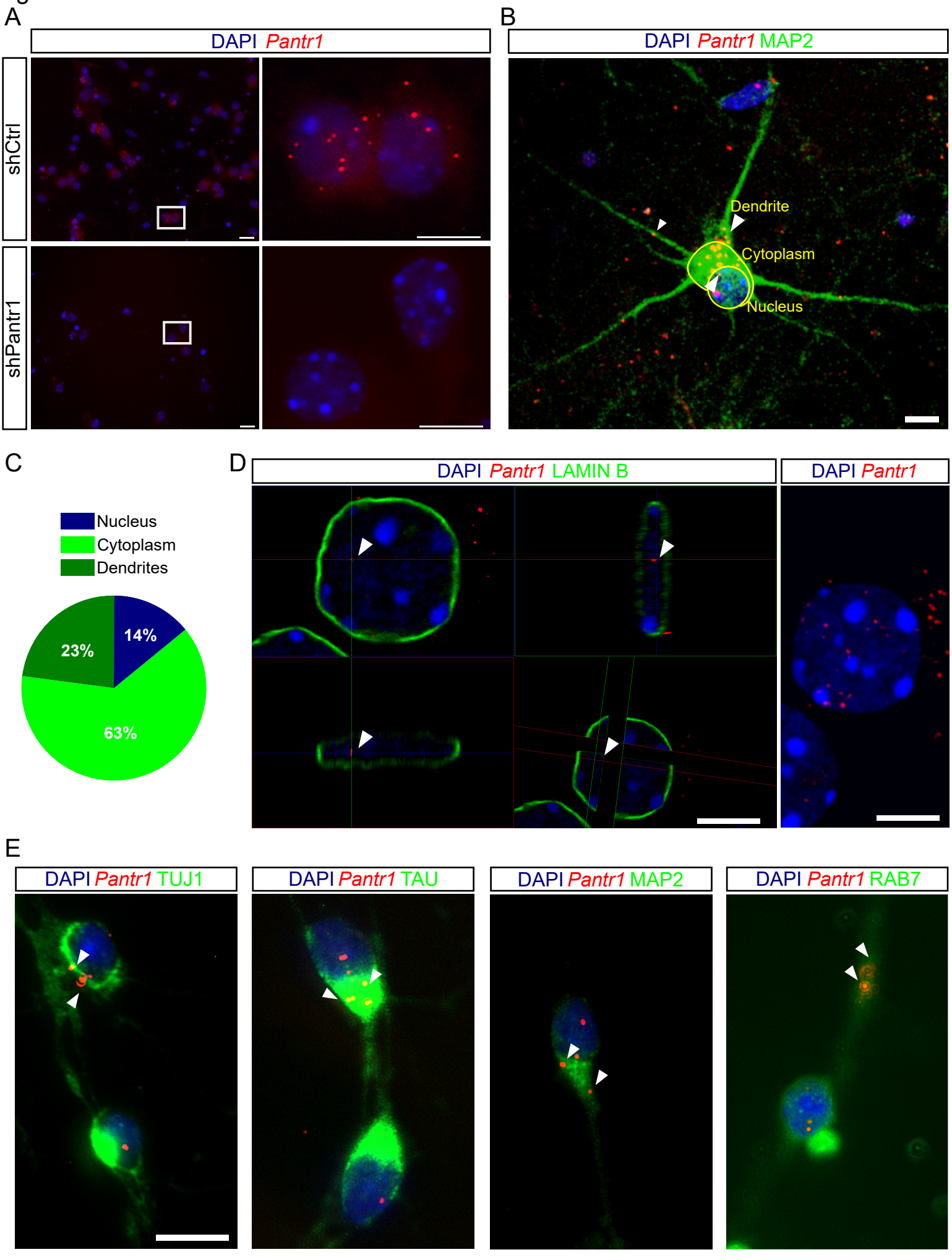

A
DAPI Pantr1
shCtrl
shPantr1
B
DAPI Pantr1 MAP2
Dendrite
Cytoplasm
Nucleus
C
Nucleus
Cytoplasm
Dendrites
14%
23%
63%
D
DAPI Pantr1 LAMIN B
DAPI Pantr1
E
DAPI Pantr1 TUJ1
DAPI Pantr1 TAU
DAPI Pantr1 MAP2
DAPI Pantr1 RAB7

Fig S4: *Pantr1* cellular localisation in hippocampal neurons

(A) SmFISH staining of *Pantr1* (red) and DAPI counterstaining (blue) in mouse DIV7 hippocampal neurons upon transduction with shCtrl or shPantr1_1. Scale bar: 20 µm. Right images show higher magnification of square in (**A)**. n=3.

(B) DIV7 primary hippocampal neurons stained with smFISH probe targeting *Pantr1* (red) and immunostained for MAP2 (green). Nuclei are marked with DAPI. *Pantr1* molecules were quantified in the delimited (arrowheads, yellow circles) cellular compartments (cytoplasm, dendrites, nucleus).

(C) Quantification of *Pantr1* dots in cells stained as illustrated in (**B)** and localising to the respective cellular compartment nucleus, cytoplasm or dendrites. n=26 cells.

(D) Left: Orthogonal projection of a confocal image of smFISH stained DIV7 hippocampal neurons showing *Pantr1* (arrowheads) inside the Lamin B-immunostained nucleus. Scale bar: 5 µm. n = 3. Right: DAPI staining and *Pantr1* smFISH in 2D representation showing *Pantr1* molecules inside and outside DAPI-positive regions.

(E) SmFISH targeting *Pantr1* combined with immunocytochemistry for TUJ1, TAU, MAP2, and RAB7 in NPCs differentiated from mouse ESCs revealed *Pantr1* localisation in axons, dendrites and late endosomes. Scale bar: 20µm, n=3.

figure S5

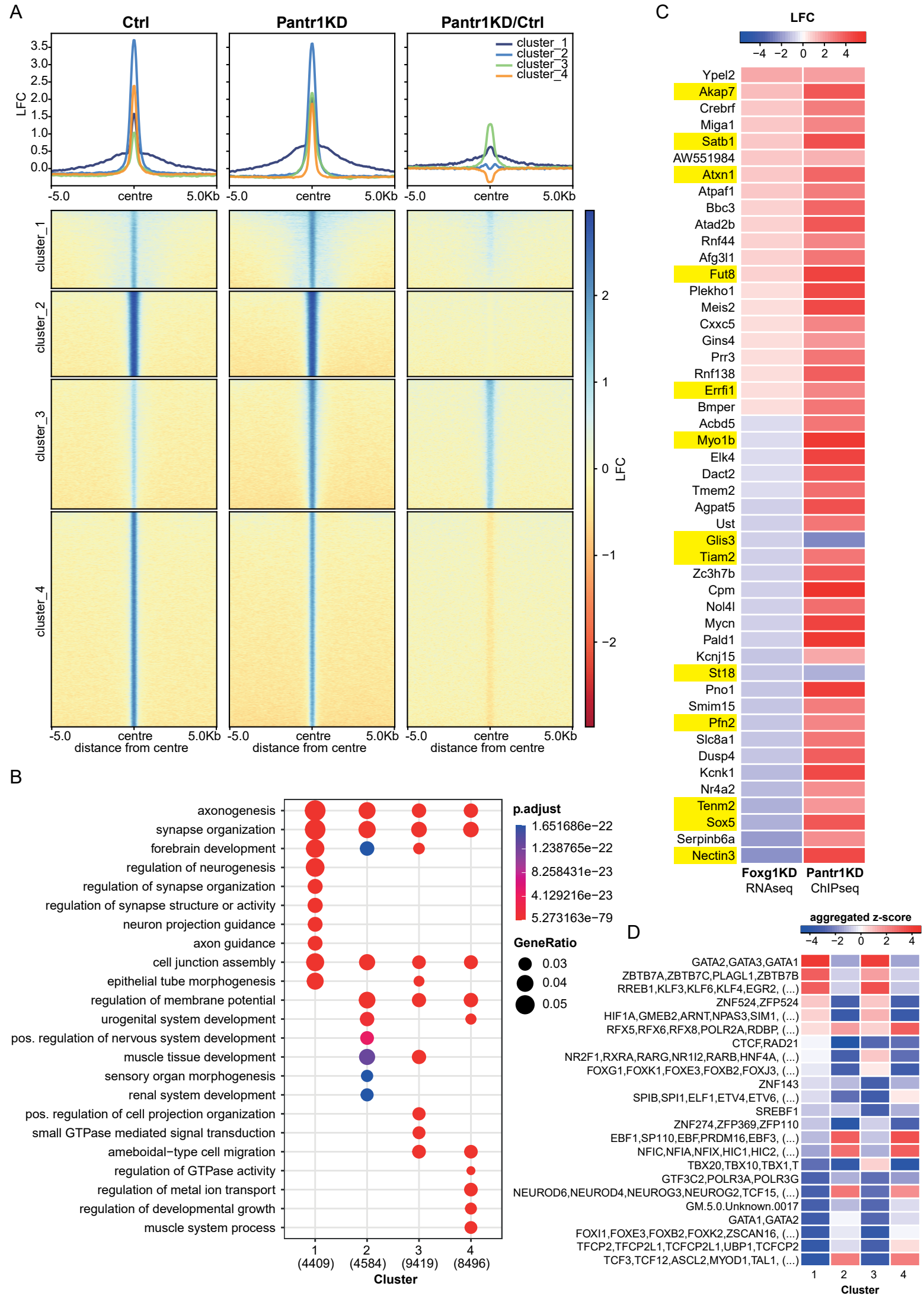

A
Ctrl
Pantr1KD
Pantr1KD/Ctrl
cluster_1
cluster_2
cluster_3
cluster_4
LFC
-5.0
centre
5.0Kb
distance from centre
B
axonogenesis
synapse organization
forebrain development
regulation of neurogenesis
regulation of synapse organization
regulation of synapse structure or activity
neuron projection guidance
axon guidance
cell junction assembly
epithelial tube morphogenesis
regulation of membrane potential
urogenital system development
pos. regulation of nervous system development
muscle tissue development
sensory organ morphogenesis
renal system development
pos. regulation of cell projection organization
small GTPase mediated signal transduction
ameboidal−type cell migration
regulation of GTPase activity
regulation of metal ion transport
regulation of developmental growth
muscle system process
p.adjust
1.651686e−22
1.238765e−22
8.258431e−23
4.129216e−23
5.273163e−79
GeneRatio
0.03
0.04
0.05
1 (4409)
2 (4584)
3 (9419)
4 (8496)
Cluster
C
LFC
Ypel2
Akap7
Crebrf
Miga1
Satb1
AW551984
Atxn1
Atpaf1
Bbc3
Atad2b
Rnf44
Afg3l1
Fut8
Plekho1
Meis2
Cxxc5
Gins4
Prr3
Rnf138
Errfi1
Bmper
Acbd5
Myo1b
Elk4
Dact2
Tmem2
Agpat5
Ust
Glis3
Tiam2
Zc3h7b
Cpm
Nol4l
Mycn
Pald1
Kcnj15
St18
Pno1
Smim15
Pfn2
Slc8a1
Dusp4
Kcnk1
Nr4a2
Tenm2
Sox5
Serpinb6a
Nectin3
Foxg1KD RNAseq
Pantr1KD ChIPseq
D
aggregated z-score
GATA2,GATA3,GATA1
ZBTB7A,ZBTB7C,PLAGL1,ZBTB7B
RREB1,KLF3,KLF6,KLF4,EGR2, (...)
ZNF524,ZFP524
HIF1A,GMEB2,ARNT,NPAS3,SIM1, (...)
RFX5,RFX6,RFX8,POLR2A,RDBP, (...)
CTCF,RAD21
NR2F1,RXRA,RARG,NR1I2,RARB,HNF4A, (...)
FOXG1,FOXK1,FOXE3,FOXB2,FOXJ3, (...)
ZNF143
SPIB,SPI1,ELF1,ETV4,ETV6, (...)
SREBF1
ZNF274,ZFP369,ZFP110
EBF1,SP110,EBF,PRDM16,EBF3, (...)
NFIC,NFIA,NFIX,HIC1,HIC2, (...)
TBX20,TBX10,TBX1,T
GTF3C2,POLR3A,POLR3G
NEUROD6,NEUROD4,NEUROG3,NEUROG2,TCF15, (...)
GM.5.0.Unknown.0017
GATA1,GATA2
FOXI1,FOXE3,FOXB2,FOXK2,ZSCAN16, (...)
TFCP2,TFCP2L1,TCFCP2L1,UBP1,TCFCP2
TCF3,TCF12,ASCL2,MYOD1,TAL1, (...)
Cluster

Fig. S5: Analyses of FOXG1-ChIPseq peaks upon *Pantr1*KD in DIV7 primary mouse hippocampal neurons

(A) Heatmap of regions 5 Kb up-/downstream of all identified FOXG1 peak summits, represented as k-means clusters with k=4 in control (Ctrl) and *Pantr1*KD condition as well as the comparison of both conditions. Data are normalised by sequencing depth and input control as log_2(ChIP/Input) for Ctrl and *Pantr1*KD data. The difference between *Pantr1*KD and control condition was calculated from RPKM normalised bigwig files as log_2 (*Pantr1*KD/Control). The metaprofiles (top) show the mean log_2FC (LFC) of each cluster. n=2.

(B) GO-term enrichment of the genes in proximity to the FOXG1 ChIPseq summits broken down to the different clusters upon *Pantr1*KD in DIV7 primary hippocampal neurons as shown in (A) with a q-value cutoff of 0.05 and p-value cutoff of 0.05.

(C) Heatmap of common DEGs in the RNAseq data sets after *Foxg1*KD (adjusted p-value (padj) < 0.05 and an LFC < -0.584 or > 0.584) and annotated genes (ChIPSeeker) corresponding to all DBRs in the FOXG1-ChIPseq data set upon *Pantr1*KD. Shown are the LFC compared to the control condition. Genes connected to neurite outgrowth and neural development are marked with a yellow box.

(D) Motif analysis of the summits in the different clusters as shown in (A). Shown is a heatmap of the aggregated z-scores.

figure S6


Nr4a2
Ust
Crebrf
Cpm
Miga1
St18
Satb1
Slc8a1
Atxn1
Dusp4
Atad2b
Afg3l1p
Rfn44
Refseq
RPKM
adult hippocampus
hipp. primary neurons
LFC
DIV7 control
DIV7 Pantr1KD
Pantr1KD/control
DBR after Pantr1KD

Fig. S6: FOXG1 binding profiles at *Pantr1*-dependent FOXG1 target genes in mouse hippocampal cells

Shown are bigwig tracks of FOXG1 binding sites upon FOXG1 ChIPseq as LFC towards input samples from murine adult hippocampus *in vivo*, and *in vitro* E18.5 cultured primary hippocampal neurons at DIV11 (hipp. primary neurons) (22), E18.5 cultured primary hippocampal neurons at DIV7 (DIV7 control) and upon *Pantr1*KD (DIV7 *Pantr1*KD) as well as the ratio of coverage upon *Pantr1*KD vs control condition (*Pantr1*KD/control). Selected genes classify as *Pantr1*-dependent FOXG1 target genes. The last track displays the binding region called as significant DBR upon *Pantr1*KD. Peak sequences of the DBRs and surrounding loci are marked with a red box. On the x-axis the position on the corresponding chromosome is indicated in bp of the mm10 genome.

figure S7

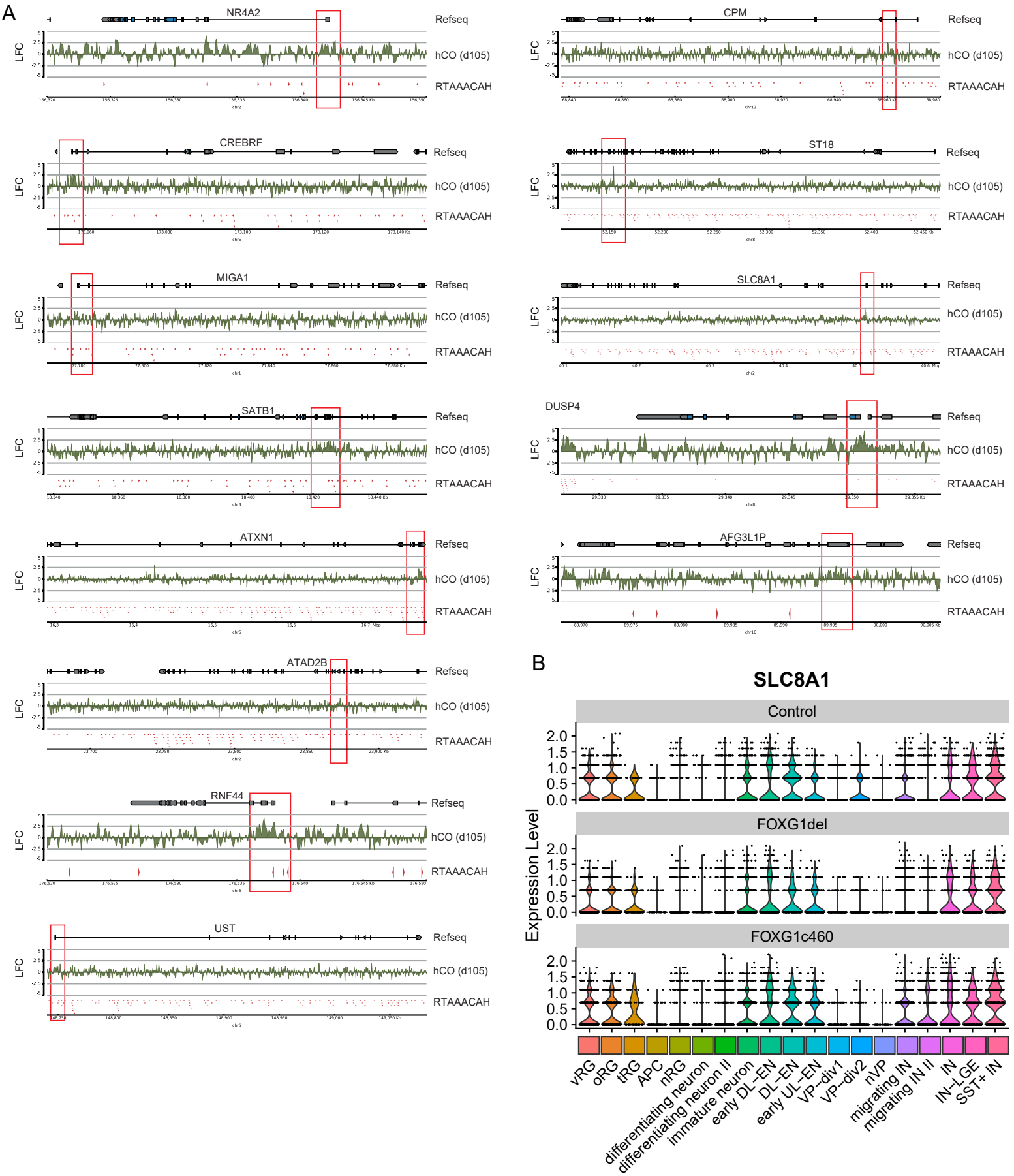

A
NR4A2
CPM
CREBRF
ST18
MIGA1
SLC8A1
SATB1
DUSP4
ATXN1
AFG3L1P
ATAD2B
RNF44
UST
Refseq
hCO (d105)
RTAAACAH
LFC
B
SLC8A1
Control
FOXG1del
FOXG1c460
Expression Level
vRG
oRG
tRG
APC
nRG
differentiating neuron
differentiating neuron II
immature neuron
early DL−EN
DL−EN
early UL−EN
VP−div1
VP−div2
nVP
migrating IN
migrating IN II
IN
IN−LGE
SST+ IN

Fig. S7: FOXG1 binding to *Pantr1*-dependent target genes in human cortical organoids

(A) ChIPseq of FOXG1 in human cortical organoids (d105, hCO) showing distribution of enriched FOXG1 peaks of the 13 mouse *Pantr1*-dependent FOXG1 target genes. Red boxes indicate the localisation of the respective DBR of FOXG1 upon *Pantr1*KD in mouse cells as shown in Fig. S6. The last track indicates predicted FOXG1 binding motifs at the respective chromosomal location. On the x-axis the position on the corresponding chromosome is indicated in bp of the hg38 genome. Mapped tracks show the $\log_2$(foldchange) (LFC) over the input sample for each condition.

(B) Violin plots of cell-type specific expression levels of *SLC8A1* in healthy donor (Control), FOXG1del, and FOXG1c460 hCO.